Model equations and parameter values.

A supplement to "A comprehensive mechanistic model of adipocyte signaling with layers of confidence"

William Lövfors[1,2], Cecilia Jönsson[1,3], Charlotta S. Olofsson[4], Elin Nyman[1,*,**], and Gunnar Cedersund[1,5, *,**]

[1]Department of Biomedical Engineering, Linköping University, Linköping, Sweden
[2]Department of Mathematics, Linköping University, Linköping, Sweden
[3]Department of Biomedical and Clinical Sciences, Linköping University, Linköping, Sweden
[4]Department of Physiology/Metabolic Physiology, Institute of Neuroscience and Physiology, The Sahlgrenska Academy at University of Gothenburg, Gothenburg, Sweden
[5]Center for Medical Image Science and Visualization (CMIV), Linköping University, Linköping, Sweden
[*]Shared last author
[**]Corresponding author

July 1, 2022

The connected model is based on ordinary differential equations (ODEs), and is a combination of three different previously published models for glucose uptake [1], adiponectin secretion [2] and lipolysis [3]. A typical ODE used in this work looks similar to Eq. (1).

$$\begin{aligned} d/dt(x) &= -va + vb \\ va &= ka \cdot x \\ vb &= kb \cdot input \end{aligned} \tag{1}$$

Here, x is a state in model, va and vb are reaction rates, ka and kb are rate determining parameters, and $input$ is some input to the state. In other words, the amount of the state x is decreased by the reaction va with the speed ka, and increased by the reaction vb with the speed kb depending on some input $input$.

In all ODEs in this document, vGx and kGx corresponds to reaction rates and rate parameters for the glucose uptake submodel, vLx and kLx to the lipolysis submodel and vAx and kAx to the adiponectin submodel. Many of the states in the model correspond to different versions of

the same thing (e.g., a phosphorylated version of a protein and an unphosphorylated version). For most of these versions, the phosphorylated/activated version spontaneously return the unphosphorylated/inactive version. These spontaneous returns to the base version will typically not be detailed.

The final connected model is shown in Fig. 3, and the equation are given in TODO. However, we will first highlight the changes made to the original submodel equations due to the connection of the submodels before we go through the equations for the connected model.

1 Connecting the submodels

For these three submodels, there are important points of crosstalk that had not previously been addressed. The glucose uptake submodel [1] and lipolysis submodel [3] have an overlap in the insulin receptor and subsequent signaling intermediaries leading up to the phosphorylation of PKB-S473 (Fig. 1). In the lipolysis model, we had previously simplified the signalling pathway from the insulin receptor to PKB as a direct interaction (action-1 in Fig. 1).

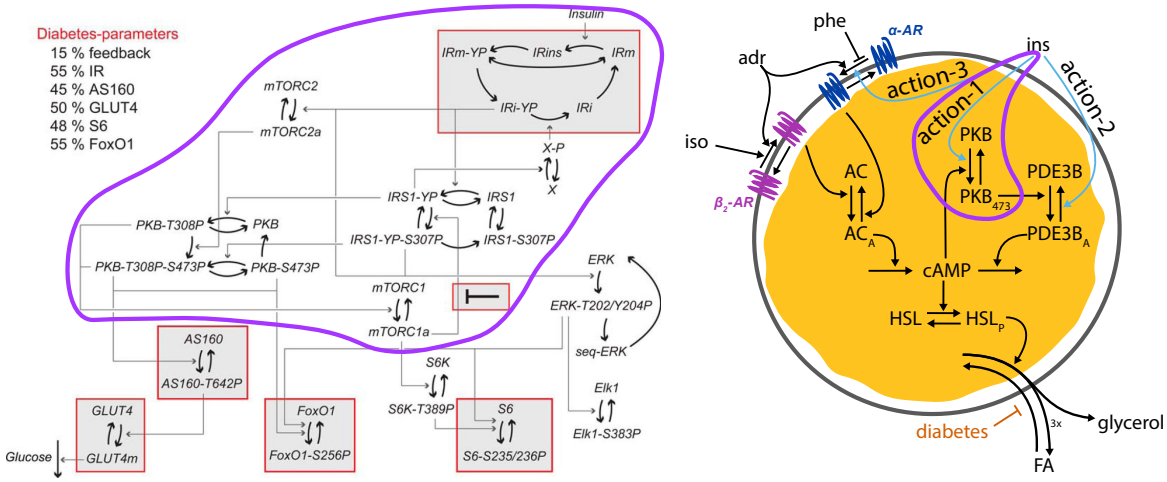

Figure 1: The glucose uptake model [1] and the lipolysis model [3]. The overlap between the models is highlighted in purple. Both model figures have previously been published under a CC-BY license.

To connect these two submodels, we updated the lipolysis submodel to use the insulin signalling pathway from the glucose uptake submodel instead of insulin action-1. In practice, we removed the equations for PKB in the lipolysis model, and changed the input to Phosphodiesterase 3B (PDE3B) from PKB_{473} as in the lipolysis model to $(PKB\_T473P + PKB\_S308P\_T473P)$ from the glucose uptake model. The equations for PDE3B used in the original lipolysis work is given in Eq. (2).

$$\begin{aligned} d/dt(PDE3B) &= -vL2a + vL2b \\ d/dt(PDE3Ba) &= vL2a - vL2b \\ vL2a &= kL2a \cdot \boldsymbol{PKB473} \cdot PDE3B \\ vL2b &= kL2b \cdot PDE3Ba \cdot Ins\_2 \end{aligned} \tag{2}$$

The updated reaction rate equations ($vL2a$, $VL2b$) for PDE3B after the models had been connected is given in Eq. (3).

$$\begin{aligned} vL2a =& kL2a \cdot (\boldsymbol{PKB\_T473P + PKB\_S308P\_T473P}) \cdot PDE3B \\ vL2b =& kL2b \cdot PDE3Ba \cdot Ins\_2 \end{aligned} \tag{3}$$

Furthermore, we added the indirect effect of cAMP on PKB (a simplified mechanism of the activation of PI3K) from the lipolysis model as an activation of mTORC2 in the pathway from the glucose uptake model, shown in bold in Eq. (4).

$$\begin{aligned} d/dt(mTORC2) &= -vG5c + vG5d \\ d/dt(mTORC2a) =& vG5c - vG5d \\ vG5c &= mTORC2 \cdot (kG5c \cdot IRi\_YP + \boldsymbol{kL1a \cdot cAMP}) \\ vG5d &= kG5d \cdot mTORC2a \end{aligned} \tag{4}$$

In addition to the overlap between the glucose uptake and lipolysis submodels, there is also an overlap between the lipolysis submodel and the adiponectin secretion submodel(Fig. 2). This overlap is cAMP.

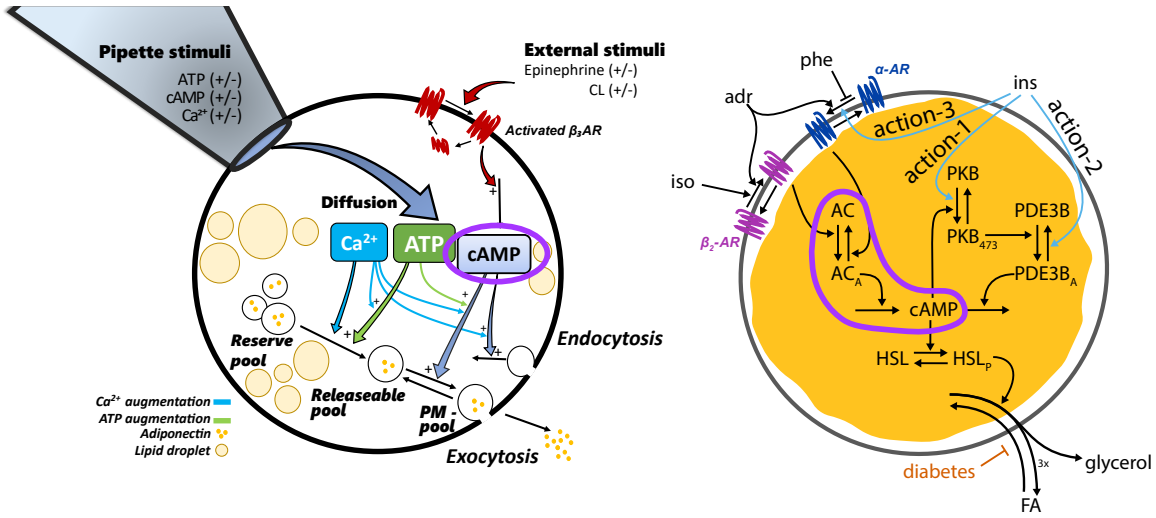

Figure 2: The adiponectin model [2] and the lipolysis model [3]. The overlap between the model is highlighted in purple. Both model figures have previously been published under a CC-BY license.

To connect the lipolysis and adiponectin submodels, we combined the reactions relating to cAMP. Furthermore, the simplified effect from the β_3 receptors to directly lead to cAMP production was instead directed to the activation of the adenylyl complex (AC) in the lipolysis submodel. The equations for cAMP from the adiponectin submodel is given in Eq. (5).

$$\begin{aligned} d/dt(cAMP) =& vApip\_cAMP + vA6a - vAdegcAMP \\ vApip\_cAMP =& kADiffcAMP \cdot (pipcAMP - cAMP) \cdot pip \\ vA6a =& kA6a \cdot BETA3a \\ vA6b =& kAdegcAMP \cdot cAMP \end{aligned} \tag{5}$$

The equations for cAMP from the lipolysis submodel is given in Eq. (6).

$$\begin{aligned} d/dt(cAMP) =& vL6a - vL6b \\ vL6a =& kL6a \cdot ACa \\ vL6b =& kL6b \cdot PDE3Ba \cdot cAMP \end{aligned} \tag{6}$$

The equations for cAMP for the connected model is given in Eq. (7).

$$\begin{aligned} d/dt(cAMP) =& vApip\_cAMP - vA6b + vL6a - vL6b \\ vApip\_cAMP =& kADiffcAMP \cdot (pipcAMP - cAMP) \cdot pip \\ vA6b =& kAdegcAMP \cdot cAMP \\ vL6a =& kL6a \cdot ACa \\ vL6b =& kL6b \cdot PDE3Ba \cdot cAMP \end{aligned} \tag{7}$$

Here it should be noted that ACa is now activated by both the β_2 receptor from the lipolysis submodel and β_3 from the adiponectin submodel. The equations for the combined AC activation is given in Eq. (8).

$$\begin{aligned} d/dt(AC) =& -vL5a + vL5b \\ d/dt(ACa) =& vL5a - vL5b + vA5a \\ vL5a =& kL5a \cdot BETA2a \cdot AC \\ vL5b =& kL5b \cdot ALPHAa \cdot ACa \\ vA5a =& kA5a \cdot BETA3a \end{aligned} \tag{8}$$

2 Description of the equations for the connected model

Here we will go through all the equations for the fully connected model Fig. 3. For readability, we will, as much as possible, go through the signalling pathways in the glucose uptake submodel first, then the lipolysis submodel and lastly the adiponectin submodel. Please note that, the model equations are explained in greater detail in the original works [1–3]. Also note that all model parameters with names starting with k are rate determining parameters, for which the parameter values are estimated based on the experimental data. These rate parameters will not be mentioned in detail below.

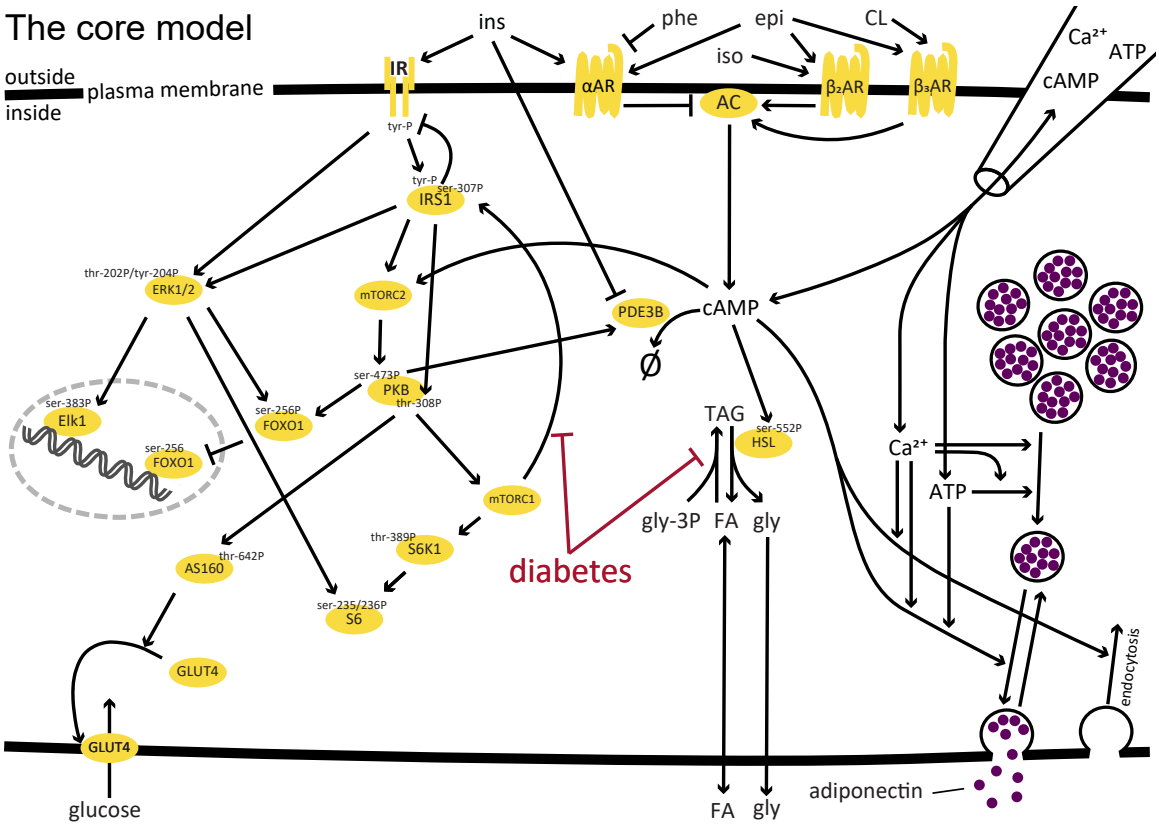

Figure 3: **The core model of adipocyte signaling**. The core model includes crosstalk between glucose uptake in response to insulin, fatty acid and glycerol release in response to alpha- and beta-adrenergic receptor signaling and adiponectin secretion in response to cAMP, ATP and Ca2+ (added into the cell with a pipette).

2.1 The glucose uptake submodel

This section describes the equations of the insulin signalling submodel, based on the model developed in [1]. Note that all reactions and parameters below are renamed from vx and kx to $v\boldsymbol{G}x$ and $k\boldsymbol{G}x$ relative to the original model in [1].

In the glucose uptake submodel, insulin binds to the insulin receptor, leading to phosphorylation of the insulin receptor. To a lesser extent, the insulin receptor can also be phosphorylated without the presence of insulin. The phosphorylated insulin receptor can either return to the unphosphorylated state directly, or be internalized. The internalized receptor will be dephosphorylated, and then return to the plasma membrane. This dephosphorylation is controlled by some unknown protein X. In the model, the states correspond to the following: IR (and IRm in Fig. 1) – the unphosphorylated insulin receptor in the plasma membrane, IR_YP – the phosphorylated insulin receptor, $IRins$ – the insulin receptor bound to insulin, IRi_YP – the internalized phosphorylated insulin receptor, and IRi – the internalized insulin receptor. The equations for the insulin receptor are described in Eq. (9).

$$
\begin{aligned}
d/dt(IR) &= -vG1a - vG1basal + vG1r + vG1g \\
d/dt(IR\_YP) &= vG1basal + vG1c - vG1d - vG1g \\
d/dt(IRins) &= vG1a - vG1c \\
d/dt(IRi\_YP) &= vG1d - vG1e \\
d/dt(IRi) &= vG1e - vG1r
\end{aligned}
$$

$$
\begin{aligned}
vG1a &= kG1a \cdot IR \cdot ins \\
vG1basal &= kG1basal \cdot IR \\
vG1c &= IRins \cdot kG1c \\
vG1d &= IR\_YP \cdot kG1d \\
vG1e &= IRi\_YP \cdot kG1f \cdot X\_P \\
vG1g &= IR\_YP \cdot kG1g \\
vG1r &= IRi \cdot kG1r
\end{aligned}
\tag{9}
$$

Downstream of the insulin receptor is the insulin receptor protein 1 (IRS1). IRS1 can be phosphorylated on tyrosine sites, and on serine 307. Note that in the model, IRS1 can be phosphorylated on both the tyrosine sites and the serine 307 site. The tyrosine phosphorylations are driven by the internalized and tyrosine phosphorylated IR, and the serine 307 phosphorylation on the already tyrosine phosphorylated IRS1 is induced by the activated mammalian target of rapamycin complex (mTORC) 1. Finally, IRS1 can spontaneously be phosphorylated on serine 307, and can spontaneously become dephosphorylated. In the model, the states correspond to: $IRS1$ – unphosphorylated IRS1, $IRS1\_YP$ – tyrosine phosphorylated IRS1, $IRS1\_S307P$, and $IRS1\_YP\_S307P$ – the IRS1 with both tyrosine phosphorylation and serine 307 phosphorylation. The equations for IRS1 are given in Eq. (10)

$$
\begin{aligned}
d/dt(IRS1) &= vG2b + vG2g - vG2a - vG2basal \\
d/dt(IRS1\_YP) &= vG2a + vG2d - vG2b - vG2c \\
d/dt(IRS1\_YP\_S307P) &= vG2c - vG2d - vG2f \\
d/dt(IRS1\_S307P) &= vG2basal + vG2f - vG2g
\end{aligned}
$$

$$
\begin{aligned}
vG2a &= IRS1 \cdot kG2a \cdot IRi\_YP \\
vG2b &= IRS1\_YP \cdot kG2b \\
vG2c &= IRS1\_YP \cdot kG2c \cdot mTORC1a \cdot diabetes \\
vG2d &= IRS1\_YP\_S307P \cdot kG2d \\
vG2f &= IRS1\_YP\_S307P \cdot kG2f \\
vG2basal &= IRS1 \cdot kG2basal \\
vG2g &= IRS1\_S307P \cdot kG2g
\end{aligned}
\tag{10}
$$

In the model, there is a protein that is still unidentified, which is denoted "protein X". This protein is a step in between IRS1 and IR, which drives the dephosphorylation of the internalized

and tyrosine phosphorylated IR. protein X is activated by the tyrosine phosphorylated IRS1. The model states correspond to: X – inactive protein x, and X_P – activated protein X. The equations for the unknown protein X are given in Eq. (11).

$$\begin{aligned} d/dt(X) &= vG3b - vG3a \\ d/dt(X\_P) &= vG3a - vG3b \\ \\ vG3a &= X \cdot kG3a \cdot IRS1\_YP \\ vG3b &= X\_P \cdot kG3b \end{aligned} \tag{11}$$

In the model, the signaling pathway leading up to the activation of mTORC2 have been simplified to a direct interaction from IR to mTORC2. mTORC2 is activated by IR that is both internalized and tyrosine phosphorylated. The model states correspond to: $mTORC2$ – inactive mTORC2, and $mTORC2a$ – activated mTORC2. The equations for mTORC2 is given in Eq. (12).

$$\begin{aligned} d/dt(mTORC2) &= -vG5c + vG5d \\ d/dt(mTORC2a) &= vG5c - vG5d \\ \\ vG5c &= mTORC2 \cdot (kG5c \cdot IRi\_YP + kL1a \cdot cAMP) \\ vG5d &= kG5d \cdot mTORC2a \end{aligned} \tag{12}$$

Downstream of IRS1 lies protein kinase B (PKB/Akt). Tyrosine phosphorylated IRS1 induces phosphorylation of PKB on threonine 308, and the dually phosphorylated IRS1 induces phosphorylation of PKB on threonine 308 on PKB already phosphorylated on serine 473. Finally, activated mTORC2 induces the serine 473 phosphorylation of PKB already phosphorylated on threonine 308. In the model, the dually phosphorylated PKB must first lose its threonine 308 phosphorylation, before the phosphorylation on serine 473 can be removed. Both single phosphorylated PKB can lose its phosphorylation. All dephosphorylations happen spontaneously. The model states corresponds to: PKB – unphosphorylated PKB, PKB_S308P – PKB phosphorylated on serine 308, PKB_T473P – PKB phosphorylated on threonine 473, and PKB_S308P_T473P – PKB phosphorylated on both serine 308 and threonine 473. The equations for PKB is given in Eq. (13).

$$
\begin{aligned}
d/dt(PKB) &= -vG4a + vG4b + vG4h \\
d/dt(PKB\_S308P) &= vG4a - vG4b - vG4c \\
d/dt(PKB\_T473P) &= -vG4e + vG4f - vG4h \\
d/dt(PKB\_S308P\_T473P) &= vG4c + vG4e - vG4f
\end{aligned}
$$

$$
\begin{aligned}
vG4a &= kG4a \cdot PKB \cdot IRS1\_YP \\
vG4b &= kG4b \cdot PKB\_S308P \\
vG4c &= kG4c \cdot PKB\_S308P \cdot mTORC2a \\
vG4e &= kG4e \cdot PKB\_T473P \cdot IRS1\_YP\_S307P \\
vG4f &= kG4f \cdot PKB\_S308P\_T473P \\
vG4h &= kG4h \cdot PKB\_T473P
\end{aligned}
\tag{13}
$$

Downstream of PKB is mTORC1. In the model, mTORC1 is activated by both PKB only phosphorylated on threonine 308, and by dually phosphorylated PKB phosphorylated on both threonine 308 and serine 473. The models states correspond to: $mTORC1$ – inactive mTORC1, and $mTORC1a$ – activated mTORC1. The equations for mTORC1 is given in Eq. (14).

$$
\begin{aligned}
d/dt(mTORC1) &= vG5b - vG5a \\
d/dt(mTORC1a) &= vG5a - vG5b
\end{aligned}
$$

$$
\begin{aligned}
vG5a &= mTORC1 \cdot (kG5a1 \cdot PKB\_S308P\_T473P + kG5a2 \cdot PKB\_S308P) \\
vG5b &= mTORC1a \cdot kG5b
\end{aligned}
\tag{14}
$$

Also, downstream of PKB is Akt substrate of 160 kDa (AS160). AS160 is phosphorylated on threonine 642 induced by PKB either phosphorylated on only serine 473 or both serine 473 and threonine 308. The model states correspond to: $AS160$ – unphosphorylated AS160, and $AS160\_T642P$ – AS160 phosphorylated on threonine 642. The equations for AS160 is given in Eq. (15).

$$
\begin{aligned}
d/dt(AS160) &= vG6b - vG6a \\
d/dt(AS160\_T642P) &= vG6a - vG6b
\end{aligned}
$$

$$
\begin{aligned}
vG6a &= AS160 \cdot (kG6a1 \cdot PKB\_S308P\_T473P + kG6a2 \cdot PKB\_T473P) \\
vG6b &= AS160\_T642P \cdot kG6b
\end{aligned}
\tag{15}
$$

AS160 when phosphorylated on threonine 642 leads to the translocation of glucose transporter 4 (GLUT4) to the plasma membrane. The model states correspond to: $GLUT4m$ – GLUT4 when translocated to the membrane, and $GLUT4$ – GLUT4 internalized in the cell. The equations for GLUT4 is given in Eq. (16).

$$
\begin{aligned}
d/dt(GLUT4m) &= vG7a - vG7b \\
d/dt(GLUT4) &= -vG7a + vG7b \\
\\
vG7a &= GLUT4 \cdot kG7a \cdot AS160\_T642P \\
vG7b &= GLUT4m \cdot kG7b
\end{aligned}
\tag{16}
$$

When GLUT4 have been translocated to the plasma membrane, it enables the uptake of glucose from the extracellular environment. In addition to the GLUT4 dependent uptake, there is also a GLUT4 independent uptake. The model state for glucose that have been taken up is $GLUCOSE$. The equation for the glucose uptake is given in Eq. (17).

$$
\begin{aligned}
d/dt(GLUCOSE) &= vG8 \\
\\
vG8 &= kG8 \cdot GLUT4m \cdot gluc/(kGmG4 + gluc) + kGglut1 \cdot gluc/(kGmG1 + gluc)
\end{aligned}
\tag{17}
$$

In addition to the glucose uptake, the *glucose uptake* model also details additional functions, such as the phosphorylation of forkhead box protein O1 (FoxO1) and ETS Like-1 protein (Elk1), via the phosphorylation of extracellular signal-regulated kinases 1/2 (ERK1/2). In the model, ERK1/2 phosphorylation on either of threonine 202 and tyrosine 204 is induced by both the internalized tyrosine phosphorylated IR and the IRS1 phosphorylated on both tyrosine sites and serine 302. After the phosphorylation of ERK1/2, it is sequestered and then returned to the unphosphorylated state. The model states correspond to: ERK – unphosphorylated ERK1/2, ERK_T202_Y204P – ERK1/2 phosphorylated on either of threonine 202 and tyrosine 204, and $seqERK$ – sequestered ERK1/2. The equations for ERK1/2 is given in Eq. (18).

$$
\begin{aligned}
d/dt(ERK) &= -vG10a - vG10basal + vG10c \\
d/dt(ERK\_T202\_Y204P) &= vG10a + vG10basal - vG10b \\
d/dt(seqERK) &= vG10b - vG10c \\
\\
vG10basal &= kG10basal \cdot ERK \\
vG10a &= kG10a1 \cdot ERK \cdot IRi\_YP + kG10a2 \cdot ERK \cdot IRS1\_YP\_S307P \\
vG10b &= kG10b \cdot ERK\_T202\_Y204P \\
vG10c &= kG10c \cdot seqERK
\end{aligned}
\tag{18}
$$

ERK1/2 when phosphorylated on either of threonine 202 and tyrosine 204, will induce the phosphorylation of Elk1 on serine 383. The model states correspond to: $Elk1$ – unphosphorylated Elk1, and $Elk1\_S383P$ – Elk1 phosphorylated on serine 383. The equations for Elk1 is given in Eq. (19).

$$
\begin{aligned}
d/dt(Elk1) &= -vG11a + vG11b \\
d/dt(Elk1\_S383P) &= vG11a - vG11b \\
\\
vG11a &= kG11a \cdot Elk1 \cdot ERK\_T202\_Y204P \\
vG11b &= kG11b \cdot Elk1\_S383P
\end{aligned}
\tag{19}
$$

In addition to Elk1, ERK1/2 also induces the phosphorylation of FoxO1 in the model. FoxO1 is phosphorylated on serine 256, induced by both Elk1/2 when phosphorylated on either of threonine 202 and tyrosine 204, and PKB phosphorylated on either tyrosine 473 or both tyrosine 473 and threonine 308. The model states correspond to: $FOXO$ – unphosphorylated FoxO1, and $FoxO1\_S256P$ – FoxO1 phosphorylated on serine 256. The equations for FoxO1 is given in Eq. (20).

$$
\begin{aligned}
d/dt(FOXO) &= -vG12a + vG12b \\
d/dt(FOXO\_S256P) &= vG12a - vG12b \\
\\
vG12a &= (kG12a1 \cdot (PKB\_T473P + PKB\_S308P\_T473P) + kG12a2 \cdot ERK\_T202\_Y204P)/ \\
vG12b &= kG12b \cdot FOXO\_S256P
\end{aligned}
\tag{20}
$$

ERK when phosphorylated on either threonine 202 or tyrosine 204, also leads to activation of the *ribosomal protein S6* (S6), in combination with the S6 kinase, *ribosomal protein S6 kinase* (S6K). In the model, S6K is phosphorylated on threonine 389, induced by the activated mTORC1a. The model states correspond to: $S6K$ – unphosphorylated S6K, and $S6K\_T389P$ – S6K phosphorylated on threonine 389. The equations for S6K is given in Eq. (21).

$$
\begin{aligned}
d/dt(S6K) &= vG9b - vG9a \\
d/dt(S6K\_T389P) &= vG9a - vG9b \\
\\
vG9a &= S6K \cdot kG9a \cdot mTORC1a \\
vG9b &= S6K\_T389P \cdot kG9b
\end{aligned}
\tag{21}
$$

In the model, S6K which is phosphorylated on threonine 389 phosphorylates S6 on serine 235 and 236. The phosphorylation of S6 is also induced by ERK phosphorylated on threonine 202 and tyrosine 204. The model states correspond to: $S6$ – unphosphorylated S6, and $S6\_S235\_S236P$ – S6 phosphorylated on any of the serine sites at 235 and 236. The equations for S6 is given in Eq. (22).

$$
\begin{aligned}
d/dt(S6) &= vG9d - vG9c \\
d/dt(S6\_S235\_S236P) &= vG9c - vG9d \\
\\
vG9c &= S6 \cdot kG9c1 \cdot S6K\_T389P + kG9c2 \cdot S6 \cdot ERK\_T202\_Y204P \\
vG9d &= S6\_S235\_S236P \cdot kG9d
\end{aligned}
\tag{22}
$$

2.2 The lipolysis submodel

This section describes the equations of the lipolysis submodel, based on the model developed in [3]. Note that all reactions and parameters below are renamed from vx and kx to $v\boldsymbol{L}x$ and $k\boldsymbol{L}x$ relative to the original model.

The lipolysis – with subsequent fatty acid and glycerol release – is in the model controlled using two different inputs: insulin which inhibits the lipolysis, and catecholamines which induce the lipolysis.

In the model, the lipolysis increasing effect of catecholamine stimulation is transmitted via the activation of the β_2 adrenergic receptor (β_2AR). In the model, the β_2AR is activated by both epinephrine (epi) and isoprenaline (iso). Due to the difference in receptor activation for the same concentration of epinephrine and isoprenaline, we introduced a scaling term for isoprenaline ($isoscale$, set to be around 10 times as strong). The model states correspond to: $BETA2$ – the inactive β_2AR, and $BETA2a$ – the activated β_2AR. The equations for the β_2 adrenergic receptor is given in Eq. (23).

$$
\begin{aligned}
d/dt(BETA2) &= -vL4a + vL4b \\
d/dt(BETA2a) &= vL4a - vL4b \\
\\
vL4a &= (kL4a \cdot (iso \cdot isoscale + epi) + kL4a2) \cdot BETA2 \\
vL4b &= kL4b \cdot BETA2a
\end{aligned}
\tag{23}
$$

In addition to the activation of the β_2AR, epinephrine also activates the α_2 adrenergic receptor (α_2AR). The α_2AR is also activated by insulin, and the activation is inhibited by the inhibitor phentolamine (phe). The model states correspond to $ALPHA2$ – the inactive α_2AR, and $ALPHA2a$ – the activated α_2AR. The equations for the αAR is given in Eq. (24).

$$
\begin{aligned}
d/dt(ALPHA) &= -vL3a + vL3b \\
d/dt(ALPHAa) &= vL3a - vL3b \\
\\
vL3a &= (kL3a \cdot Ins\_3 \cdot epi + kL3a2) \cdot (1 - phe\_effect \cdot phe) \cdot ALPHA \\
vL3b &= kL3b \cdot ALPHAa
\end{aligned}
\tag{24}
$$

Activation of the β_2AR leads to activation of the adenylyl cyclase (AC), and activation of the α_2AR deactivates AC. Additionally, AC can be activated by the β_3 adrenergic receptor (β_3AR), which is also activated by epinephrine and was originally part of the adiponectin submodel (not detailed yet). The model states correspond to: AC - inactive AC, and ACa - active AC. The equations for the adenylyl cyclase is given in Eq. (25).

$$\begin{aligned}
d/dt(AC) &= -vL5a + vL5b \\
d/dt(ACa) &= vL5a - vL5b + vA5a \\
\\
vL5a &= kL5a \cdot BETA2a \cdot AC \\
vL5b &= kL5b \cdot ALPHAa \cdot ACa \\
vA5a &= kA5a \cdot BETA3a
\end{aligned} \tag{25}$$

When AC is activated, it will lead to the production of cAMP. In addition to the production, cAMP will also be degraded. In the model, this is done either passively of by activated PDE3B. Finally, in the model, cAMP can also diffuse between the cytosol and an attached pipette if a patch-clamp experiment is simulated (originally part of the adiponectin submodel, and not detailed yet). The equation for cAMP is given in Eq. (26).

$$\begin{aligned}
d/dt(cAMP) &= vL6a - vL6b - vA6b + vApip_cAMP \\
\\
vL6a &= kL6a \cdot ACa \\
vL6b &= kL6b \cdot PDE3Ba \cdot cAMP \\
vA6b &= kAdegcAMP \cdot cAMP \\
vApip_cAMP &= kADiffcAMP \cdot (pipcAMP - cAMP) \cdot pip
\end{aligned} \tag{26}$$

As mentioned, the degradation of cAMP is controlled by PDE3B. The activation of PDE3B is in turn induced via PKB phosphorylated on either only threonin 473, or phosphorylated on both threonine 473 and serine 308, originally induced by insulin stimulation. Furthermore, there is another insulin action at high concentrations of insulin that leads to the deactivation of PDE3B (Eq. (30), Ins_2). The model states correspond to: $PDE3B$ - inactive PDE3B, and $PDE3Ba$ - activated PDE3B. The equations for PDE3B is given in Eq. (27).

$$\begin{aligned}
d/dt(PDE3B) &= -vL2a + vL2b \\
d/dt(PDE3Ba) &= vL2a - vL2b \\
\\
vL2a &= kL2a \cdot (PKB_T473P + PKB_S308P_T473P) \cdot PDE3B \\
vL2b &= kL2b \cdot PDE3Ba \cdot Ins_2
\end{aligned} \tag{27}$$

When the cAMP levels rise, it triggers a signaling cascade leading to the activation of lipases that hydrolyze the triacylicglycerides (TAGs) into fatty acids (FAs) and glycerol. In the model, this signaling cascade is simplified as only the activation of HSL. In the model, HSL

phosphorylation on serine 552 is induced by the increased levels of cAMP. The model states correspond to: HSL - unphosphorylated HSL, and $HSLp$ - HSL phosphorylated on serine 552. The equations for HSL is given in Eq. (28).

$$\begin{aligned} d/dt(HSL) &= -vL7a + vL7b \\ d/dt(HSLp) &= vL7a - vL7b \\ \\ vL7a &= kL7a \cdot cAMP \cdot HSL \\ vL7b &= kL7b \cdot HSLp \end{aligned} \tag{28}$$

Once HSL is activated, it will lead to the breakdown of TAGs into fatty acids and glycerol which are subsequently released. Both fatty acids and glycerol will be cleared away from the extracellular environment in the *in vivo* setting, but not in the *in vitro* setting. Some fatty acids will be reesterified into TAGs again. In the model, the pool of TAGs is assumed to be unchanged during the timescale of the model simulations. Furthermore, the glycerol-3P needed to reform TAGs from FAs are also assumed to be unlimited. The model states correspond to: Gly - released glycerol, and FA - released fatty acids. The equations for the release of glycerol and fatty acids is given in Eq. (29). Note that $kLclear$ was set to 0 in the *in vitro* setting.

$$\begin{aligned} d/dt(Gly) &= vL8a - vL8b \\ d/dt(FA) &= 3 \cdot vL8a - vL8c \\ \\ vL8a &= kL8a \cdot HSLp \\ vL8b &= kLclear \cdot Gly \\ vL8c &= (kLclear + kL8c \cdot diab\_reest) \cdot FA \end{aligned} \tag{29}$$

We modelled the other two insulin actions described in the works by Jönsson et al. [4] and Stich et al. [5] as two separate sigmoidal functions, both dependent on the concentration of insulin. The dose dependent insulin actions are given in Eq. (30).

$$\begin{aligned} Ins_2 &= 100 + \frac{min_2 - 100}{1 + (ins/EC50_2)^{n_2}} \\ Ins_3 &= 100 + \frac{min_3 - 100}{1 + (ins/EC50_3)^{n_3}} \end{aligned} \tag{30}$$

2.3 The adiponectin submodel

This section describes the equations of the lipolysis submodel, based on the model developed in [2]. Note that all reactions and parameters below are renamed from vx and kx to $v\boldsymbol{A}x$ and $k\boldsymbol{A}x$ relative to the original model.

In the model, vesicles containing adiponectin is moved from a large reserve pool of vesicles, to a releasable pool, and is then attached to the plasma membrane. Finally, the vesicles can undergo exocytosis. The experimental data, and thus the model measurement equation, is the

membrane capacitance which corresponds to the size of the cell. The size is increased when vesicles undergo exocytosis. The size can also shrink during endocytosis. The exocytosis and endocytosis is controlled by the intracellular mediators cAMP, Ca^{2+} and ATP. cAMP have previously been discussed as a part of the lipolysis submodel (Eq. (26)). In the context of the adiponectin submodel, cAMP can also be produced as a result of the activation of the β_3 adrenergic receptor (β_3AR) and controlled directly via a patch-clamp experiment. In the patch-clamp experiment, cAMP is infused in the cell using the attached pipette, and the cAMP levels can thus be controlled.

The β_3 adrenergic receptor (β_3AR) is activated by epinephrine and the synthetic analogue CL 316,243 (CL). The activated β_3AR will then be desensitized before returning to the inactive state. The model states correspond to: $BETA3$ – inactive (β_3AR), $BETA3a$ – activated (β_3AR), and $BETA3de$ – desensitized (β_3AR). The equations for the β_3AR is given in Eq. (31).

$$\begin{aligned}
d/dt(BETA3) &= vA4c - vA4a \\
d/dt(BETA3a) &= vA4a - vA4b \\
d/dt(BETA3de) &= vA4b - vA4c \\
\\
vA4a &= kA4a \cdot (epi + kACL \cdot CL) \cdot BETA3 \\
vA4b &= kA4b \cdot BETA3a \\
vA4c &= kA4c \cdot BETA3de
\end{aligned} \tag{31}$$

In addition to cAMP, two other intracellular mediators were controlled using the patch-clamp setup: Ca^{2+} and ATP. All mediators can diffuse between the pipette and the intracellular environment, and then can be removed from the intracellular environment (by being sequestered, degraded, etc.). Due to the large differences in the volume of the pipette and the cell, the concentration change in the pipette due to diffusion was scaled as a fraction of the cell volume and the pipette volume ($kAVcell/kAVpip$). The model states correspond to: Ca – intracellular Ca^{2+}, $cAMP$ – intracellular cAMP, $pipCa$ – Ca^{2+} in the pipette, $pipATP$ – ATP in the pipette, and $pipcAMP$ – cAMP in the pipette. The equations for the intracellular mediators Ca^{2+} and ATP, and the pipette, is given in Eq. (32).

$$
\begin{aligned}
d/dt(Ca) &= vApip\_Ca - vAremCa \\
d/dt(ATP) &= vApip\_ATP - vAdegATP \\
\\
d/dt(pipCa) &= -vApip\_Ca \cdot kAVcell/kAVpip \\
d/dt(pipATP) &= -vApip\_ATP \cdot kAVcell/kAVpip \\
d/dt(pipcAMP) &= -vApip\_cAMP \cdot kAVcell/kAVpip \\
\\
vApip\_Ca &= kADiffCa \cdot (pipCa - Ca) \cdot pip \\
vApip\_ATP &= kADiffATP \cdot (pipATP - ATP) \cdot pip \\
vAremCa &= kAremCa \cdot Ca \\
vAdegATP &= kAdegATP \cdot ATP \\
vApip\_cAMP &= kADiffcAMP \cdot (pipcAMP - cAMP) \cdot pip
\end{aligned}
\tag{32}
$$

The reserve pool of vesicles (Res) was assumed to not change during the short timescale of the adiponectin release experiments. The equation for the reserve pool is given in Eq. (33).

$$
d/dt(Res) = 0 \tag{33}
$$

The vesicles will migrate from the reserve pool to a releasable pool, augmented by Ca^{2+} and ATP. Then, the releasable vesicles will attach to the plasma membrane, controlled by cAMP and augmented by Ca^{2+} and ATP. The vesicles attached to the plasma membrane can then undergo exocytosis or return to the releasable pool. The model states correspond to: Rel – the releasable pool, and PM - the vesicles attached to the plasma membrane. The equations for releasable pool is given in Eq. (34).

$$
\begin{aligned}
d/dt(Rel) &= vARes\_Rel - vARel\_PM + vAPM\_Rel \\
d/dt(PM) &= vARel\_PM - vAPM\_Rel - vAPM \\
\\
vARes\_Rel &= ((Ca/(kAm + Ca)) \cdot (kACa2 + kAATP2 \cdot ATP) + kARelBasal) \cdot Res \\
vARel\_PM &= cAMP \cdot (kAcAMP + (Ca/(kAm + Ca)) \cdot ATP \cdot kACaATP) \cdot Rel \\
vAPM\_Rel &= kArel \cdot PM \\
vAPM &= kAexo \cdot PM
\end{aligned}
\tag{34}
$$

In addition to the exocytosis, cAMP also induces endocytosis. The endocytosis is also augmented by Ca^{2+}. The equation for the endocytosis is given in Eq. (35)

$$
d/dt(Endo) = vACa\_Endo - vAEndo \tag{35}
$$

The vesicles undergoing exocytosis leads to increased levels of adiponectin in the extracellular environment. Since the experiments are *in vitro*, we assume that no adiponectin is cleared. Also, we assume that the released adiponectin will diffuse too far away form the cell to be affected by the endocytosis. The equation for the released adiponectin is given in Eq. (36).

$$\begin{aligned} d/dt(Adiponectin) =& vAPM \\ \\ vACa\_Endo \quad =& kACacAMP \cdot cAMP \cdot Ca \\ vAEndo \quad =& kAEndo \cdot Endo \end{aligned} \tag{36}$$

3 Parameter values

This section gives the optimal parameter values for the connected model both when estimated to the estimation data set (columns θ^*_{est}), and to the total data set (columns θ^*_{tot}). Furthermore, the bounds used in the optimization for all parameters are also given (columns *lowerbound* and *upperbound*). The parameter values and optimization bounds for the glucose uptake submodel are given in Table 1 and Table 2. The parameter values and optimization bounds for the lipolysis submodel are given in Table 3. The parameter values and optimization bounds for the adiponectin submodel are given in Table 4.

Parameter	θ^*_{est}	θ^*_{tot}	lower bound	upper bound
$kG1a$	$1.2696 \cdot 10^{-1}$	$1.2501 \cdot 10^{-1}$	$1.0000 \cdot 10^{-8}$	$1.0000 \cdot 10^{6}$
$kG1basal$	$2.2526 \cdot 10^{-4}$	$2.2526 \cdot 10^{-4}$	$1.0000 \cdot 10^{-8}$	$1.0000 \cdot 10^{6}$
$kG1c$	$1.7234 \cdot 10^{-1}$	$1.7224 \cdot 10^{-1}$	$1.0000 \cdot 10^{-8}$	$1.0000 \cdot 10^{6}$
$kG1d$	$9.9995 \cdot 10^{5}$	$9.9997 \cdot 10^{5}$	$1.0000 \cdot 10^{-8}$	$1.0000 \cdot 10^{6}$
$kG1f$	$2.0184 \cdot 10^{1}$	$2.0267 \cdot 10^{1}$	$1.0000 \cdot 10^{-8}$	$1.0000 \cdot 10^{6}$
$kG1g$	$5.3850 \cdot 10^{-8}$	$3.1332 \cdot 10^{-8}$	$1.0000 \cdot 10^{-8}$	$1.0000 \cdot 10^{6}$
$kG1r$	6.5382	6.4662	$1.0000 \cdot 10^{-8}$	$1.0000 \cdot 10^{6}$
$kG2a$	$7.2702 \cdot 10^{1}$	$7.2938 \cdot 10^{1}$	$1.0000 \cdot 10^{-8}$	$1.0000 \cdot 10^{6}$
$kG2c$	$2.0619 \cdot 10^{3}$	$2.0024 \cdot 10^{3}$	$1.0000 \cdot 10^{-8}$	$1.0000 \cdot 10^{6}$
$kG2basal$	$7.2956 \cdot 10^{-2}$	$7.1708 \cdot 10^{-2}$	$1.0000 \cdot 10^{-8}$	$1.0000 \cdot 10^{6}$
$kG2b$	$3.7448 \cdot 10^{3}$	$3.7448 \cdot 10^{3}$	$1.0000 \cdot 10^{-8}$	$1.0000 \cdot 10^{6}$
$kG2d$	4.8589	4.8512	$1.0000 \cdot 10^{-8}$	$1.0000 \cdot 10^{6}$
$kG2f$	$9.1342 \cdot 10^{-1}$	$9.1327 \cdot 10^{-1}$	$1.0000 \cdot 10^{-8}$	$1.0000 \cdot 10^{6}$
$kG2g$	$2.9109 \cdot 10^{-1}$	$2.8790 \cdot 10^{-1}$	$1.0000 \cdot 10^{-8}$	$1.0000 \cdot 10^{6}$
$kG3a$	$8.6395 \cdot 10^{1}$	$8.5992 \cdot 10^{1}$	$1.0000 \cdot 10^{-8}$	$1.0000 \cdot 10^{6}$
$kG3b$	$1.0026 \cdot 10^{-1}$	$1.0452 \cdot 10^{-1}$	$1.0000 \cdot 10^{-8}$	$1.0000 \cdot 10^{6}$
$kG4a$	$6.7328 \cdot 10^{2}$	$6.7328 \cdot 10^{2}$	$1.0000 \cdot 10^{-8}$	$1.0000 \cdot 10^{6}$
$kG4b$	$9.6161 \cdot 10^{4}$	$9.6157 \cdot 10^{4}$	$1.0000 \cdot 10^{-8}$	$1.0000 \cdot 10^{6}$
$kG4c$	$6.2629 \cdot 10^{3}$	$6.1511 \cdot 10^{3}$	$1.0000 \cdot 10^{-8}$	$1.0000 \cdot 10^{6}$
$kG4e$	$4.8452 \cdot 10^{-2}$	$4.8419 \cdot 10^{-2}$	$1.0000 \cdot 10^{-8}$	$1.0000 \cdot 10^{6}$
$kG4f$	7.7143	7.3032	$1.0000 \cdot 10^{-8}$	$1.0000 \cdot 10^{6}$
$kG4h$	$9.1781 \cdot 10^{-2}$	$9.1778 \cdot 10^{-2}$	$1.0000 \cdot 10^{-8}$	$1.0000 \cdot 10^{6}$
$kG5a1$	3.0828	2.9201	$1.0000 \cdot 10^{-8}$	$1.0000 \cdot 10^{6}$
$kG5a2$	$1.3173 \cdot 10^{4}$	$1.3540 \cdot 10^{4}$	$1.0000 \cdot 10^{-8}$	$1.0000 \cdot 10^{6}$
$kG5b$	$2.3183 \cdot 10^{1}$	$2.3184 \cdot 10^{1}$	$1.0000 \cdot 10^{-8}$	$1.0000 \cdot 10^{6}$
$kG5d$	$1.4851 \cdot 10^{-1}$	$1.4851 \cdot 10^{-1}$	$1.0000 \cdot 10^{-8}$	$1.0000 \cdot 10^{6}$
$kG5c$	6.4703	6.3330	$1.0000 \cdot 10^{-8}$	$1.0000 \cdot 10^{6}$
$kG6a1$	$1.9667 \cdot 10^{-1}$	$1.9198 \cdot 10^{-1}$	$1.0000 \cdot 10^{-8}$	$1.0000 \cdot 10^{6}$
$kG6a2$	$1.1012 \cdot 10^{-7}$	$1.0513 \cdot 10^{-7}$	$1.0000 \cdot 10^{-8}$	$1.0000 \cdot 10^{6}$
$kG6b$	$2.2643 \cdot 10^{-1}$	$2.3368 \cdot 10^{-1}$	$1.0000 \cdot 10^{-8}$	$1.0000 \cdot 10^{6}$
$kG7a$	$2.5980 \cdot 10^{-6}$	$2.6309 \cdot 10^{-6}$	$1.0000 \cdot 10^{-8}$	$1.0000 \cdot 10^{6}$
$kG7b$	$1.6018 \cdot 10^{3}$	$1.6330 \cdot 10^{3}$	$1.0000 \cdot 10^{-8}$	$1.0000 \cdot 10^{6}$
$kG8$	$3.7913 \cdot 10^{4}$	$3.8195 \cdot 10^{4}$	$1.0000 \cdot 10^{-8}$	$1.0000 \cdot 10^{6}$
$kGglut1$	$2.0747 \cdot 10^{-2}$	$2.0805 \cdot 10^{-2}$	$1.0000 \cdot 10^{-8}$	$1.0000 \cdot 10^{6}$
$kGmG4$	$1.1159 \cdot 10^{1}$	$1.1071 \cdot 10^{1}$	$1.0000 \cdot 10^{-8}$	$1.0000 \cdot 10^{6}$
$kGmG1$	$8.8508 \cdot 10^{-1}$	$8.8402 \cdot 10^{-1}$	$1.0000 \cdot 10^{-8}$	$1.0000 \cdot 10^{6}$
$kG9a$	$1.1660 \cdot 10^{-6}$	$1.1786 \cdot 10^{-6}$	$1.0000 \cdot 10^{-8}$	$1.0000 \cdot 10^{6}$
$kG9b$	$4.9870 \cdot 10^{-2}$	$4.9403 \cdot 10^{-2}$	$1.0000 \cdot 10^{-8}$	$1.0000 \cdot 10^{6}$
$kG9c1$	$4.2332 \cdot 10^{-1}$	$4.1739 \cdot 10^{-1}$	$1.0000 \cdot 10^{-8}$	$1.0000 \cdot 10^{6}$
$kG9c2$	$1.9737 \cdot 10^{-2}$	$1.9038 \cdot 10^{-2}$	$1.0000 \cdot 10^{-8}$	$1.0000 \cdot 10^{6}$
$kG9d$	$3.2024 \cdot 10^{-2}$	$3.2662 \cdot 10^{-2}$	$1.0000 \cdot 10^{-8}$	$1.0000 \cdot 10^{6}$

Table 1: **Parameter values.**

$kG10a1$	$9.4534 \cdot 10^{-7}$	$2.4530 \cdot 10^{-7}$	$1.0000 \cdot 10^{-8}$	$1.0000 \cdot 10^{6}$
$kG10a2$	$8.2693 \cdot 10^{-4}$	$8.3407 \cdot 10^{-4}$	$1.0000 \cdot 10^{-8}$	$1.0000 \cdot 10^{6}$
$kG10basal$	$9.5726 \cdot 10^{-3}$	$9.5430 \cdot 10^{-3}$	$1.0000 \cdot 10^{-8}$	$1.0000 \cdot 10^{6}$
$kG10b$	$1.8650 \cdot 10^{-1}$	$1.8514 \cdot 10^{-1}$	$1.0000 \cdot 10^{-8}$	$1.0000 \cdot 10^{6}$
$kG10c$	$2.5402 \cdot 10^{-4}$	$2.5572 \cdot 10^{-4}$	$1.0000 \cdot 10^{-8}$	$1.0000 \cdot 10^{6}$
$kG11a$	$9.2964 \cdot 10^{-8}$	$9.2595 \cdot 10^{-8}$	$1.0000 \cdot 10^{-8}$	$1.0000 \cdot 10^{6}$
$kG11b$	$3.9138 \cdot 10^{-1}$	$3.9123 \cdot 10^{-1}$	$1.0000 \cdot 10^{-8}$	$1.0000 \cdot 10^{6}$
$kG12a1$	$1.0188 \cdot 10^{3}$	$1.0328 \cdot 10^{3}$	$1.0000 \cdot 10^{-8}$	$1.0000 \cdot 10^{6}$
$kG12a2$	$4.9313 \cdot 10^{5}$	$4.9310 \cdot 10^{5}$	$1.0000 \cdot 10^{-8}$	$1.0000 \cdot 10^{6}$
$kG12b$	$1.9751 \cdot 10^{1}$	$1.9997 \cdot 10^{1}$	$1.0000 \cdot 10^{-8}$	$1.0000 \cdot 10^{6}$
$kGm12$	$1.7943 \cdot 10^{4}$	$1.7943 \cdot 10^{4}$	$1.0000 \cdot 10^{-8}$	$1.0000 \cdot 10^{6}$
$diabetes$	$5.5870 \cdot 10^{-2}$	$5.6831 \cdot 10^{-2}$	0	1.0000

Table 2: **Parameter values related to the glucose uptake submodel.**

$kLdrift$	$2.3544 \cdot 10^{2}$	$2.3859 \cdot 10^{2}$	$1.0000 \cdot 10^{-8}$	$1.0000 \cdot 10^{6}$
$kL1a$	6.3543	6.5066	$1.0000 \cdot 10^{-8}$	$1.0000 \cdot 10^{6}$
$kL2a$	$2.0167 \cdot 10^{-2}$	$2.0173 \cdot 10^{-2}$	$1.0000 \cdot 10^{-8}$	$1.0000 \cdot 10^{6}$
$kL2b$	$1.5134 \cdot 10^{-2}$	$1.5133 \cdot 10^{-2}$	$1.0000 \cdot 10^{-8}$	$1.0000 \cdot 10^{6}$
$kL3b$	$2.6030 \cdot 10^{3}$	$2.6139 \cdot 10^{3}$	$1.0000 \cdot 10^{-8}$	$1.0000 \cdot 10^{6}$
$kL3a$	$1.3271 \cdot 10^{2}$	$1.4695 \cdot 10^{2}$	$1.0000 \cdot 10^{-8}$	$1.0000 \cdot 10^{6}$
$kL3a2$	$2.5765 \cdot 10^{2}$	$2.5765 \cdot 10^{2}$	$1.0000 \cdot 10^{-8}$	$1.0000 \cdot 10^{6}$
$kL4a$	$1.1421 \cdot 10^{-2}$	$1.1415 \cdot 10^{-2}$	$1.0000 \cdot 10^{-8}$	$1.0000 \cdot 10^{6}$
$kL4a2$	$2.3029 \cdot 10^{-4}$	$2.3122 \cdot 10^{-4}$	$1.0000 \cdot 10^{-8}$	$1.0000 \cdot 10^{6}$
$kL4b$	2.1055	2.1060	$1.0000 \cdot 10^{-8}$	$1.0000 \cdot 10^{6}$
$kL5a$	$2.5570 \cdot 10^{-1}$	$2.5654 \cdot 10^{-1}$	$1.0000 \cdot 10^{-8}$	$1.0000 \cdot 10^{6}$
$kL5b$	7.5766	7.5763	$1.0000 \cdot 10^{-8}$	$1.0000 \cdot 10^{6}$
$kL6a$	$8.4296 \cdot 10^{-2}$	$8.4395 \cdot 10^{-2}$	$1.0000 \cdot 10^{-8}$	$1.0000 \cdot 10^{6}$
$kL6b$	$2.3022 \cdot 10^{-2}$	$2.3084 \cdot 10^{-2}$	$1.0000 \cdot 10^{-8}$	$1.0000 \cdot 10^{6}$
$kL7a$	$7.2582 \cdot 10^{2}$	$9.0592 \cdot 10^{2}$	$1.0000 \cdot 10^{-8}$	$1.0000 \cdot 10^{6}$
$kL7b$	$1.3458 \cdot 10^{1}$	$1.2935 \cdot 10^{1}$	$1.0000 \cdot 10^{-8}$	$1.0000 \cdot 10^{6}$
$kL8a$	$2.9542 \cdot 10^{2}$	$2.6349 \cdot 10^{2}$	$1.0000 \cdot 10^{-8}$	$1.0000 \cdot 10^{6}$
$kL8c$	$2.2077 \cdot 10^{-2}$	$2.5507 \cdot 10^{-2}$	$1.0000 \cdot 10^{-8}$	$1.0000 \cdot 10^{6}$
$kLclear$	$3.7677 \cdot 10^{-2}$	$3.6746 \cdot 10^{-2}$	$1.0000 \cdot 10^{-8}$	$1.0000 \cdot 10^{6}$
$isoscale$	$1.2000 \cdot 10^{1}$	$1.2000 \cdot 10^{1}$	8.0000	$1.2000 \cdot 10^{1}$
phe_effect	$8.9227 \cdot 10^{-1}$	$8.8912 \cdot 10^{-1}$	$6.0000 \cdot 10^{-1}$	1.0000
$min2$	$2.0854 \cdot 10^{1}$	$2.0854 \cdot 10^{1}$	0	$1.0000 \cdot 10^{2}$
$min3$	$9.8712 \cdot 10^{-3}$	$9.8712 \cdot 10^{-3}$	0	$1.0000 \cdot 10^{2}$
$EC502$	1.0882	1.0720	-5.0000	3.0000
$EC503$	$8.2934 \cdot 10^{-2}$	$6.6394 \cdot 10^{-2}$	-5.0000	3.0000
$n2$	3.0000	2.1674	$5.0000 \cdot 10^{-1}$	3.0000
$n3$	3.0000	2.9723	$5.0000 \cdot 10^{-1}$	3.0000
$diab\_reest$	$9.6659 \cdot 10^{-2}$	$1.2111 \cdot 10^{-1}$	0	1.0000

Table 3: **Parameter values related to the lipolysis submodel.**

$kArel$	$2.0500 \cdot 10^{-7}$	$3.2440 \cdot 10^{-7}$	$1.0000 \cdot 10^{-8}$	$1.0000 \cdot 10^{6}$
$kAexo$	$6.6957 \cdot 10^{-1}$	$6.6957 \cdot 10^{-1}$	$1.0000 \cdot 10^{-8}$	$1.0000 \cdot 10^{6}$
$kACaATP$	$2.9179 \cdot 10^{1}$	$2.9226 \cdot 10^{1}$	$1.0000 \cdot 10^{-8}$	$1.0000 \cdot 10^{6}$
$kAcAMP$	$1.8864 \cdot 10^{1}$	$1.8864 \cdot 10^{1}$	$1.0000 \cdot 10^{-8}$	$1.0000 \cdot 10^{6}$
$kACa2$	$1.1695 \cdot 10^{-3}$	$1.1638 \cdot 10^{-3}$	$1.0000 \cdot 10^{-8}$	$1.0000 \cdot 10^{6}$
$kAATP2$	$9.2660 \cdot 10^{-4}$	$9.2651 \cdot 10^{-4}$	$1.0000 \cdot 10^{-8}$	$1.0000 \cdot 10^{6}$
$kAEndo$	$8.0992 \cdot 10^{5}$	$9.9826 \cdot 10^{5}$	$1.0000 \cdot 10^{-8}$	$1.0000 \cdot 10^{6}$
$kACacAMP$	$6.0089 \cdot 10^{2}$	$6.0768 \cdot 10^{2}$	$1.0000 \cdot 10^{-8}$	$1.0000 \cdot 10^{6}$
kAm	$1.2535 \cdot 10^{-8}$	$1.2535 \cdot 10^{-8}$	$1.0000 \cdot 10^{-8}$	$1.0000 \cdot 10^{6}$
$kARelBasal$	$1.0534 \cdot 10^{-4}$	$1.0749 \cdot 10^{-4}$	$1.0000 \cdot 10^{-8}$	$1.0000 \cdot 10^{6}$
$kAdegcAMP$	$2.0201 \cdot 10^{-6}$	$1.8269 \cdot 10^{-6}$	$1.0000 \cdot 10^{-8}$	$1.0000 \cdot 10^{6}$
$kAremCa$	$5.5039 \cdot 10^{-5}$	$4.8329 \cdot 10^{-5}$	$1.0000 \cdot 10^{-8}$	$1.0000 \cdot 10^{6}$
$kAdegATP$	$2.2781 \cdot 10^{-1}$	$2.4347 \cdot 10^{-1}$	$1.0000 \cdot 10^{-8}$	$1.0000 \cdot 10^{6}$
$kADiffcAMP$	$2.7110 \cdot 10^{-1}$	$2.7104 \cdot 10^{-1}$	$1.0000 \cdot 10^{-8}$	$1.0000 \cdot 10^{6}$
$kADiffCa$	$1.6417 \cdot 10^{4}$	$1.6417 \cdot 10^{4}$	$1.0000 \cdot 10^{-8}$	$1.0000 \cdot 10^{6}$
$kADiffATP$	$5.3773 \cdot 10^{-1}$	$4.9675 \cdot 10^{-1}$	$1.0000 \cdot 10^{-8}$	$1.0000 \cdot 10^{6}$
$kA4a$	$1.7383 \cdot 10^{4}$	$1.7384 \cdot 10^{4}$	$1.0000 \cdot 10^{-8}$	$1.0000 \cdot 10^{6}$
$kACL$	$2.4186 \cdot 10^{-5}$	$2.4874 \cdot 10^{-5}$	$1.0000 \cdot 10^{-8}$	$1.0000 \cdot 10^{6}$
$kA4c$	$1.0638 \cdot 10^{-8}$	$1.0001 \cdot 10^{-8}$	$1.0000 \cdot 10^{-8}$	$1.0000 \cdot 10^{6}$
$kA4b$	2.8284	2.8344	$1.0000 \cdot 10^{-8}$	$1.0000 \cdot 10^{6}$
$kA5a$	3.2559	3.2559	$1.0000 \cdot 10^{-8}$	$1.0000 \cdot 10^{6}$
$kAVpip$	$2.2330 \cdot 10^{-5}$	$2.3223 \cdot 10^{-5}$	$2.0000 \cdot 10^{-5}$	$6.0000 \cdot 10^{-5}$
$kAVcell$	$1.6689 \cdot 10^{-13}$	$1.6613 \cdot 10^{-13}$	$8.6400 \cdot 10^{-15}$	$1.7168 \cdot 10^{-13}$

Table 4: **Parameter values related to the adiponectin submodel.**

4 Initial values

The model was given arbitrary initial values and then simulated without any inputs until steady state was reached to get a stable set of inti before any experiment was started. In most cases, the values are expressed as percentages. In other words, all state of a component in the model sum to 100. Note that the initial values for the mediators in the pipett ($pipCa$, $pipcAMP$, and $pipATP$) was set to the corresponding experimental concentrations during the start of the simulation of the adiponectin experiments (after steady state), and was set to 0 during all other experiments. The initial values used - before simulation to steady state - are given in Table 5, Table 6, and Table 7 for the glucose uptake, lipolysis, and adiponectin submodels respectively.

State	Initial values
IR	100
IR_YP	0
$IRins$	0
IRi_YP	0
IRi	0
$IRS1$	100
$IRS1\_YP$	0
$IRS1\_YP\_S307P$	0
$IRS1\_S307P$	0
X	100
X_P	0
PKB	100
PKB_S308P	0
PKB_T473P	0
PKB_S308P_T473P	0
$mTORC1$	100
$mTORC1a$	0
$mTORC2$	100
$mTORC2a$	0
$AS160$	100
$AS160\_T642P$	0
$GLUT4m$	0
$GLUT4$	100
$GLUCOSE$	0
$S6K$	100
$S6K\_T389P$	0
$S6$	100
$S6\_S235\_S236P$	0
ERK	100
ERK_T202_Y204P	0
$seqERK$	0
$Elk1$	100
$Elk1\_S383P$	0
$FOXO$	100
$FOXO\_S256P$	0

Table 5: **Initial values for the glucose uptake submodel.**

$BETA2$	100
$BETA2a$	0
$ALPHA$	80
$ALPHAa$	20
AC	80
ACa	20
$PDE3B$	80
$PDE3Ba$	20
$cAMP$	0
HSL	80
$HSLp$	20
Gly	0
FA	0

Table 6: **Initial values for the lipolysis submodel.**

$BETA3$	100
$BETA3a$	0
$BETA3de$	0
Ca	0
ATP	0
Res	99
Rel	1
PM	0
$Endo$	0
$Adiponectin$	0
$pipCa$	0
$pipATP$	0
$pipcAMP$	0

Table 7: **Initial values for the adiponectin submodel.**

References

1. Rajan, M. R., Nyman, E., Kjølhede, P., Cedersund, G. & Strålfors, P. Systems-Wide Experimental and Modeling Analysis of Insulin Signaling through Forkhead Box Protein O1 (FOXO1) in Human Adipocytes, Normally and in Type 2 Diabetes. *Journal of Biological Chemistry* **291,** 15806–15819 (July 22, 2016).
2. Lövfors, W. *et al.* A Systems Biology Analysis of Adrenergically Stimulated Adiponectin Exocytosis in White Adipocytes. *Journal of Biological Chemistry* **297** (Nov. 1, 2021).
3. Lövfors, W. *et al.* A Systems Biology Analysis of Lipolysis and Fatty Acid Release from Adipocytes in Vitro and from Adipose Tissue in Vivo. *PLOS ONE* **16,** e0261681 (Dec. 31, 2021).

4. Jönsson, C., Castor Batista, A. P., Kjølhede, P. & Strålfors, P. Insulin and β-Adrenergic Receptors Mediate Lipolytic and Anti-Lipolytic Signalling That Is Not Altered by Type 2 Diabetes in Human Adipocytes. *Biochemical Journal* **476,** 2883–2908 (Oct. 15, 2019).

5. Stich, V. *et al.* Activation of A2-Adrenergic Receptors Blunts Epinephrine-Induced Lipolysis in Subcutaneous Adipose Tissue during a Hyperinsulinemic Euglycemic Clamp in Men. *American Journal of Physiology-Endocrinology and Metabolism* **285,** E599–E607 (Sept. 1, 2003).